



Antidiabetic and Antioxidant Activity of Green Synthesized Starch Nanoparticles: An In Vitro Study

Vishnupriyan Varadharaj¹ · Arulvel Ramaswamy² · Rajeswari Sakthivel¹ · Ramasamy Subbaiya² · Hamed Barabadi³ · Murugesan Chandrasekaran⁴ · Muthupandian Saravanan⁵

Received: 18 October 2019 / Published online: 20 November 2019
© Springer Science+Business Media, LLC, part of Springer Nature 2019

Abstract

This study was aimed to assess the antidiabetic and antioxidant activity of starch nanoparticles (StNPs) synthesized by green synthesis through in vitro model. Several organic solvents were used for the extraction of active compounds from *Gymnema sylvestre*. The methanolic extract was used for the synthesis of StNPs from dried potato starch. The characterization studies such as GC–MS, FT-IR, SEM, EDS and XRD were performed to analyze the sample. The StNPs were found to be ellipsoidal in nature with the average particle size of 19.8 nm. The StNPs showed highest DPPH radical scavenging activity with $74.41 \pm 0.54\%$ at 100 $\mu\text{g/mL}$ concentration. Besides, the IC_{50} values were found to be 66.69 $\mu\text{g/mL}$ and 61.99 $\mu\text{g/mL}$ for the StNPs and standard (ascorbic acid), respectively. The StNPs showed the highest metal ion chelating activity of $66.71 \pm 0.34\%$ at a concentration of 100 $\mu\text{g/mL}$. The highest reducing power of StNPs was found to be 0.385 ± 0.002 at 100 $\mu\text{g/mL}$. Moreover, in vitro antidiabetic activity was studied using alpha-amylase inhibition assay and the highest inhibition activity of StNPs was $58.56 \pm 0.44\%$ at a concentration of 100 $\mu\text{g/mL}$. The present study provided preliminary evidence indicated that the StNPs synthesized using methanolic extract of *G. sylvestre* had potential activity against diabetes.

Keywords Biosynthesis · Starch nanoparticles · *Gymnema sylvestre* · Bioactive compounds · Antidiabetic · Antioxidant

Introduction

Nanoscience and nanotechnology refer to the study and application of materials at nanoscale in different areas including biology, chemistry, physics, medicine, etc. [1, 2]. An estimated US\$ 75.8 Billion has been anticipated for the

global nanotechnology industry by 2020 [2]. Nanomaterials have specific behaviors and unique physicochemical properties in comparison to their bulk materials and have large surface area to volume ratio [3]. The unique properties of nanomaterials have attracted significant attentions for their pharmaceutical applications [4–8]. Different characteristics of nanomaterials such as morphology, size

✉ Arulvel Ramaswamy
arulvelbabooo@gmail.com

✉ Muthupandian Saravanan
bioinfosaran@gmail.com;
saravanan.muthupandian@mu.edu.et

¹ Department of Biotechnology, K.S.Rangasamy College of Technology, Namakkal (District), Tiruchengode, Tamil Nadu 637 215, India

² Department of Biotechnology, Saveetha School of Engineering, Saveetha Institute of Medical and Technical Sciences, Saveetha Nagar, Chennai, Tamil Nadu 602105, India

³ Department of Pharmaceutical Biotechnology, School of Pharmacy, Shahid Beheshti University of Medical Sciences, Tehran, Iran

⁴ Department of Food Science and Biotechnology, Sejong University, Seoul, Republic of Korea

⁵ Department of Medical Microbiology and Immunology, Division of Biomedical Science, School of Medicine, College of Health Sciences, Mekelle University, Mekelle, Ethiopia

distribution, surface chemistry and surface charge may change their physicochemical properties and consequently their pharmaceutical efficacy [9–11]. Nanomaterials can be synthesized through different methods such as chemical [1], physical [12] and biological methods [13–17]. The biological approach for preparation of nanomaterials has emerged highlighted interest in recent years due to their simplicity, eco-friendliness, and cost effectiveness [18]. The biological mediated synthesis of nanomaterials is ecofriendly benign due to the lack of hazard chemicals compared to chemical methods that use toxic reagents though their procedures [18, 19]. Nanomaterials prepared from natural polysaccharides, are bio-compatible, non-toxic, and bio-degradable. Besides, the natural polysaccharides are easily available in nature [20, 21].

Starch is a natural polysaccharide composed of amylose and amylopectin. StNPs synthesized by nanotechnological process have attracted more attention in recent years because they afford greater opportunity for mass production and are non-hazardous to human health. StNPs were produced using nanoprecipitation method from the starch solution and were found in the range of 132 to 220 nm in diameter with the concentration of the maize starch increased from 2.5 to 10% [22]. Diabetes is a condition noticeable by high levels of glucose raised from the problems in imbalance of insulin production. People with diabetes might develop serious complications such as heart diseases, stroke, kidney failure, blindness, and premature death [23]. The leaves of *Gymnema sylvestre* have the mixture of bioactive compounds such as terpenes, saponins, gymnemic acid, gymnemagenin and gumarin. Due to the presence of these bioactive compounds, this plant shows anti-diabetic activity. This plant is also known as ‘Sugar destroyer’. Its leaves are also used in food additives against obesity. Besides, its root is used as an antidote for snake bites by tribal [24]. The current research focused on the preparation of StNPs using *G. sylvestre* using green approach and evaluating its anti-diabetic and anti-oxidant activity through in vitro model.

Materials and Methods

Sample Collection and Extraction

The plant *G. sylvestre* was procured from the local villages of Tiruchengode, Namakkal, India during the month of August 2016. The plant sample were washed with tap water and shade dried for further use. The dried sample was powdered and extracted using various solvents through increasing polarity such as toluene, benzene, chloroform, ethyl acetate, methanol and water. 10 g of sample was extracted using 100 mL of solvents and the process was

carried out for 24 h in an orbital shaker. The extract was then filtered using filter paper and stored at room temperature.

Phytochemical Analysis

The preliminary phytochemical analysis was done by the method described elsewhere [25]. The extracts were intended to the preliminary analysis for the detection of alkaloids, flavonoids, saponins, tannins, coumarins, phenols, carbohydrates, glycosides, reducing sugars and proteins.

Starch Nanoparticle Synthesis

The StNPs were synthesized through the method described elsewhere [22] with some modifications. Briefly, 5 g of dried potato starch was added to 100 mL of distilled water. The mixture was kept at room temperature for 150 min under continuous mechanical stirring till the formation of homogeneous solution. To this solution, 20 mL of plant extract was added drop-wise under continuous vigorous mechanical stirring. The solution was stirred for 4 h until the solution becomes clear. Then, it was centrifuged at 10000 rpm for 20 min. The supernatant was removed and the settled nanoparticles were purified using distilled water and 70% ethanol which removes water and unreacted compounds. The StNPs solution was freeze dried using a lyophilizer. The lyophilized StNPs were stored in a container for further analysis and testing.

Characterization Studies of StNPs

The characterisations of biosynthesised StNPs were performed by Fourier Transform Infra-red Spectroscopy (FT-IR), Scanning Electron Microscopy (SEM), Energy-Dispersive X-Ray Spectroscopy (EDS), X-ray Powder Diffraction (XRD), and Particle Size Analysis.

Alpha-Amylase Inhibition Assay

Alpha-amylase inhibition assay was done using DNSA method as stated by Olubomethin et al. [26]. The inhibition of alpha-amylase was calculated by the following formula,

$$\alpha\text{-amylase inhibition activity (\%)} = \frac{A_0 - A_1}{A_0} \times 100$$

where A_0 is the absorbance of the control (blank, without StNPs) and A_1 is the absorbance of the sample.

Metal Ion Chelating Assay

Metal ion chelating activity was determined by the method described by Dinis et al. [27]. The standard solution used was EDTA (2 mM). The chelating activity of the StNPs for Fe^{2+} was expressed as:

$$\text{Iron chelating activity (\%)} = \frac{A_0 - A_1}{A_0} \times 100$$

where A_0 is the absorbance of the control (blank, without StNPs) and A_1 is the absorbance of the sample.

2, 2-Diphenyl-1-Picryl Hydrazyl (DPPH) Assay

This test was measured as described by Blois [28] and Hatano et al. [29] with slight modifications. The free radical scavenging activity of each fraction was determined by comparing its absorbance with blank solution (no sample). The ability to scavenge the DPPH radical was calculated using the following formula,

$$\text{DPPH scavenging activity (\%)} = \frac{A_0 - A_1}{A_0} \times 100$$

where A_0 is the absorbance of the control (blank, without StNPs) and A_1 is the absorbance of the sample.

Glucose Uptake by Yeast Cells

This method was performed as stated by Cirillo et al. [30]. The percentage increase in glucose uptake by yeast cells was calculated using the following formula,

$$\text{Glucose uptake (\%)} = \frac{A_1 - A_0}{A_1} \times 100$$

where A_0 is the absorbance of the control (blank, without StNPs) and A_1 is the absorbance of the sample.

Reducing Power Assay

Reducing power was determined by the method described by Oyaizu et al. [31] with some minor modifications. A stronger absorbance indicates increased reducing power.

Results and Discussions

Phytochemical Analysis

The preliminary tests for the different phytochemicals were performed as per the standard protocol (Fig. 1). It was found that toluene extract has no effect on elution. The coumarins were detected by the observation of yellow color. The pattern of blue green or red coloration indicated

the presence of quinones. The formation of violet ring showed the presence of carbohydrates. The alkaloids and coumarins were present in the ethyl acetate extract. Alkaloids, flavonoids, saponins, tannins, phenols, coumarins, and proteins were present in the methanol extract. As methanol is the solvent of high polarity, most of the compounds were eluted. The water extract contained the alkaloids, flavonoids, saponins, and proteins. These biomolecules play a role in synthesis and stabilization of green StNPs.

GC–MS Analysis

The GC–MS examination on the methanolic leaf extract of *G. sylvestre* was used to assess the bioactive components present in the extract. GC analysis revealed the presence of 6 dominant bioactive components. Figure 2 showed the gas chromatogram of the methanolic extract of *G. sylvestre*. The major compounds identified were 2, 2-Diethyl butanoic acid, 1, 2, 3, 4-cyclohexanetetrol *N*-hexadecanoic acid, (1R)-(-)-trans-pinane-1, 10-diol, 3, 4'-dimethoxybiphenyl. The compound 4, 4, 6a, 6b, 8a, 11, 11, 14b-octamethyl-1, 4, 4a, 5, 6, 6a, 6b, 7, 8, 8a, 9, 10, 11, 12, 12a, 14, 14a, 14b-octadecahydro-2 was almost similar to the commercially available compound 9(11), 12-Oleanadien-3-ol with the molecular formula of $\text{C}_{30}\text{H}_{48}\text{O}$.

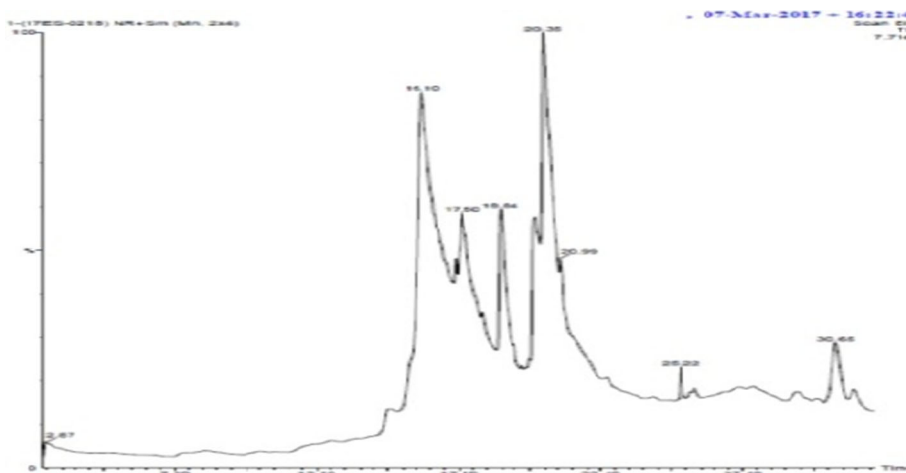
SEM and PSA Analysis

The morphological features of the starch particles were investigated by SEM and PSA analysis to understand the structure of StNPs. The SEM image showed the topology of the StNPs. Based on the SEM results, the StNPs were found to be ellipsoidal in shape (Fig. 3). In comparison with StNPs, the native starch was found to be polygonal in shape with the size about 2–20 μm [22]. This was due to that starch molecules may contain large amount of amylose



Fig. 1 Various solvent extracts of *Gymnema sylvestre*

Fig. 2 Gas chromatogram of the methanolic extract of *Gymnema sylvestre*



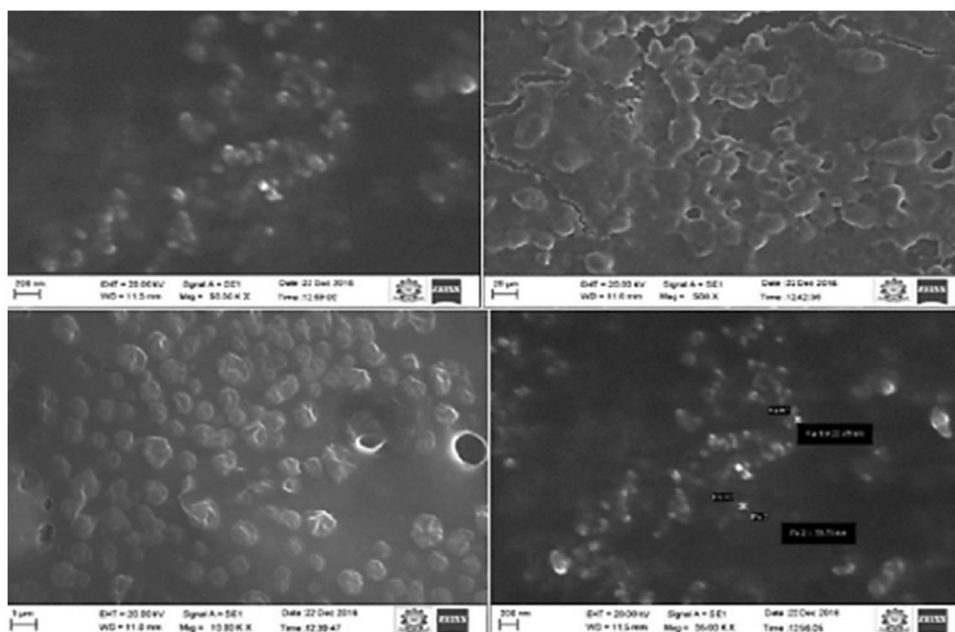
and amylopectin, but in addition of the solvent, it disrupted the bonding between the molecules and breaks into small molecules. It was observed from SEM image, that the nanoparticles obtained were non-homogeneous and aggregated in nature. The particle size analysis showed the nanoparticles ranges within the size between 2 and 200 nm with an average size of 19.8 nm.

FT-IR Analysis

FT-IR was used to determine the functional group present in the sample. The Fig. 4a, b demonstrated the methanolic extract of *G. sylvestre* and FT-IR peaks of the StNPs. In StNPs, the characteristic functional groups of amylopectin were observed in 1639 to 3250 cm^{-1} . Hebeish et al. [22] reported that the same characteristic band was observed for

the native starch which was highly rich in the amylose and amylopectin. The wide band observed at 3348 cm^{-1} can be attributed to the O–H stretching of the amylopectin and its width was described to the formation of inter and intramolecular hydrogen bonds. The bands at 2935 and 2887 cm^{-1} were recognized as asymmetric stretching of C–H, while the peak at 1656 cm^{-1} was ascribed to adsorbed water and the bands at 1421 and 1357 cm^{-1} correspond to the angular deformation of C–H. The C–O ether bond shows stretching at 1156 cm^{-1} , while the C–O alcohol bond shows stretching at 1015 cm^{-1} . The peak at 2260 cm^{-1} represents stretching of N–C=O group, the low intensity peak at 1600 and 3400 cm^{-1} were probably caused by vibrations of the NH bonds, the band at 1726 cm^{-1} represents stretching of C=O group; the one at 1100 cm^{-1} was caused by stretching of the C–O group.

Fig. 3 SEM image of StNPs under different magnifications



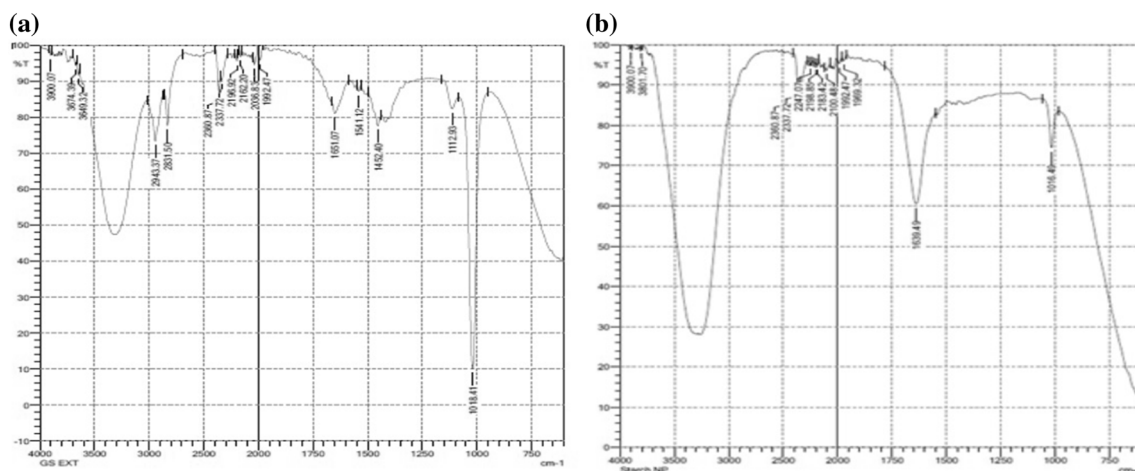


Fig. 4 **a** FT-IR spectra for methanolic extract of *Gymnema sylvestre*. **b** FT-IR spectra for StNPs

The band at 2870 cm^{-1} represents stretching vibration of the C–H group, the one at 2970 cm^{-1} was caused by stretching of the C–H (CH_3) group, the band at 1370 cm^{-1} represents deformation of the C–H bond and the bands at 1537 and 1450 cm^{-1} represents three-substituted benzene ring.

EDS Analysis

The energy dispersive X-ray spectroscopy is an analytical technique used for the elemental analysis of the sample. The electrons generated by the electron gun are accelerated and it irradiates the StNPs. The kinetic energy dissipated within the StNPs generate the signals. These signals are the information used for EDS study. The incident electrons have energy to strike the inner shell of the atom and it form an electron hole. The electron from the outer shell fills up the hole and emits the X-rays. These characteristic X-rays comprises the different energy for each element and the intensity indirectly proportional to the element concentration. The Fig. 5 showed the EDS spectrum of the StNPs and the results indicated the incidence of carbon, nitrogen, oxygen, sodium, chlorine and sulphur. Considering StNPs, the higher percentage of carbon indicate the occurrence of plant extract within the StNPs. The plant extract contains amine compounds which have nitrogen in it. Sulphur is due to the presence of proteins and amino acids such as cysteine present in the plant extract. The presence of sodium and chlorine is perhaps due to the presence of sodium and chloride ions in the extract or due to the contaminants in chemical reagents.

XRD Analysis

The X-ray diffraction analysis determines the crystallinity or amorphous nature of the StNPs. Starch is a

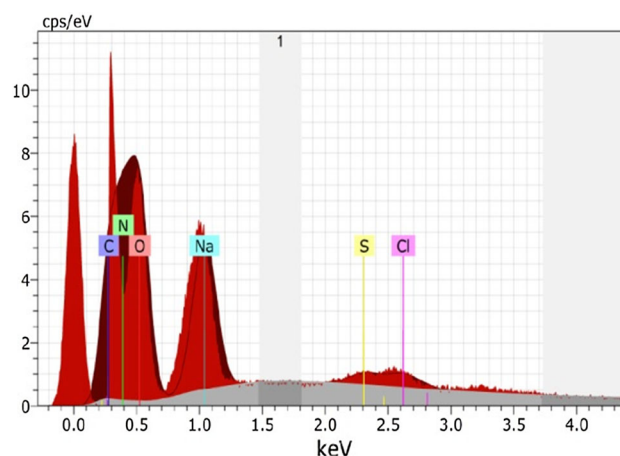


Fig. 5 EDS spectrum of the synthesized StNPs

polysaccharide which contains semi-crystalline granules with various polymorphic type and it differs in degree of crystallinity. X-ray diffraction is based on the Bragg's law. According to the previous report by Haaj et al. [32], the native starch exhibited the diffraction pattern with the peaks at Bragg's angle (2θ) at about 15° , 23° , 17° and 18° . As, the particle size of the native starch were large, the starch showed crystalline structure. The size of the crystallite becomes smaller, as the particle size decreases and get the broader diffraction peak as shown in Fig. 6. The StNPs were formed by the precipitation of starch solution using the methanolic extract results in the disruption of the crystalline structure of the clustered amylopectin, which formed the StNPs with the low intensity and more amorphous in nature with the diffraction peak at 2θ value of 28.8° .

DPPH Assay

Antioxidants are compounds which prevents the oxidation of molecules. The oxidative stress is caused due to the imbalance between antioxidants and reactive oxygen species, which leads to the death and damage of the cells. The reaction between antioxidant molecules and DPPH radical, results in decrease in absorbance at 517 nm. The results revealed that the StNPs showed highest DPPH radical scavenging activity of $74.41 \pm 0.54\%$ at $100 \mu\text{g/mL}$ concentration followed by $60.56 \pm 0.23\%$, $42.23 \pm 1.05\%$, $29.97 \pm 0.48\%$, $19.22 \pm 0.59\%$ at concentrations of $80 \mu\text{g/mL}$, $60 \mu\text{g/mL}$, $40 \mu\text{g/mL}$ and $20 \mu\text{g/mL}$, respectively. The antioxidant capacity was expressed as 50% inhibitory concentration (IC_{50}). The IC_{50} was calculated from the standard curve of StNPs and it was found to be $66.69 \mu\text{g/mL}$. The IC_{50} was calculated from the standard curve of standard (ascorbic acid) and it was found to be $61.99 \mu\text{g/mL}$. The similar report was stated by Kalyani et al. [33] that the ethanolic extract of *G. sylvestre* revealed the maximum scavenging activity with $83.41 \pm 0.13\%$ at $120 \mu\text{g/mL}$ concentration which was more significant to that of $100 \mu\text{g/mL}$ concentration of StNPs with $74.41 \pm 0.54\%$ DPPH radical scavenging activity. Phenolic compounds present in the StNPs may be responsible for the variation in the antioxidant activity. It was perceived that the antioxidant values were increased with increase in the concentration of StNPs (Fig. 7).

Metal Ion Chelating Assay

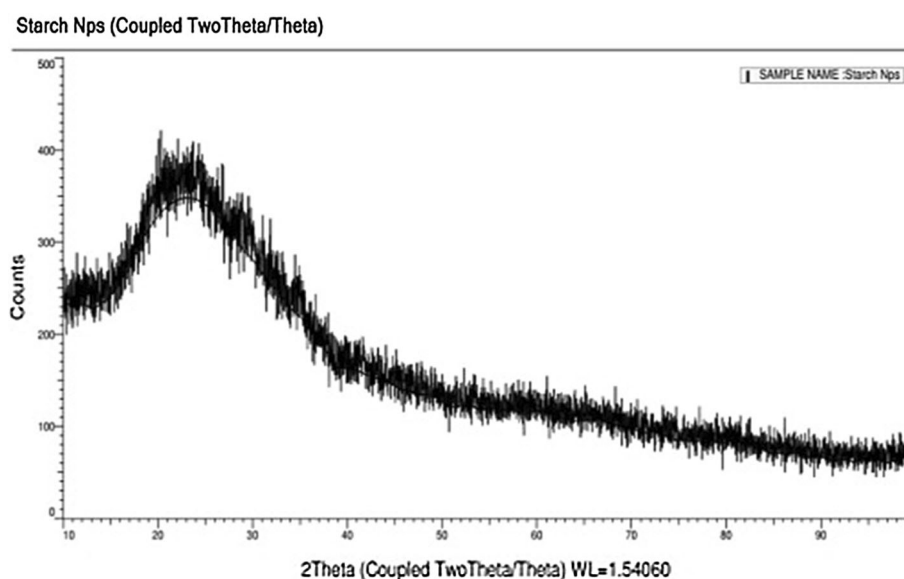
The retardation of metal-catalyzed oxidation renders important anti-oxidative effects due to chelation of ferrous ion. Iron is the most important lipid pro-oxidant and highly

reactive amongst all transition metals. The iron can excite lipid peroxidation by Fenton's reaction. On reaction with Fe^{2+} , ferrozine forms magenta complexes. The formation of complexes is disrupted due the presence of chelating agents, which results in complex decrease in absorbance with decrease in color. This shows higher metal chelating activity. The results revealed that the StNPs showed the highest metal ion chelating activity with $66.71 \pm 0.34\%$ at $100 \mu\text{g/mL}$ concentration followed by $49.08 \pm 0.61\%$, $25.53 \pm 0.30\%$, $18.43 \pm 0.52\%$, and $15.87 \pm 0.31\%$ at concentrations of $80 \mu\text{g/mL}$, $60 \mu\text{g/mL}$, $40 \mu\text{g/mL}$, and $20 \mu\text{g/mL}$, respectively. The standard showed the metal ion chelating activity with $79.84 \pm 0.25\%$, $66.02 \pm 0.47\%$, $49.26 \pm 0.38\%$, $31.96 \pm 0.28\%$, and $18.76 \pm 0.53\%$ at concentrations of $100 \mu\text{g/mL}$, $80 \mu\text{g/mL}$, $60 \mu\text{g/mL}$, $40 \mu\text{g/mL}$, and $20 \mu\text{g/mL}$, respectively. Figure 8 described the graphical representation of metal chelating activity. The antioxidant capacity is expressed as 50% inhibitory concentration (IC_{50}). The IC_{50} was calculated from the standard curve of StNPs and it was found to be $82.48 \mu\text{g/mL}$. The IC_{50} was calculated from the standard curve of standard (EDTA) and it was found to be $61.07 \mu\text{g/mL}$.

Reducing Power Assay

Flavonoids are a large and diversified class of compounds which exist widely in plants with a range of properties including antioxidant, anti-mutagenic, anti-carcinogenic effects. The reducing power of the StNPs and the standard (ascorbic acid) were evaluated. The free radicals can receive an electron from the antioxidant which lead to the neutralization of the radical. The electron donation in the reduction of $\text{Fe}^{3+}(\text{CN})_6-\text{Fe}^{2+}(\text{CN})_6$ leads to measurement of the reducing power. This was observed by the

Fig. 6 XRD spectrum of the synthesized StNPs



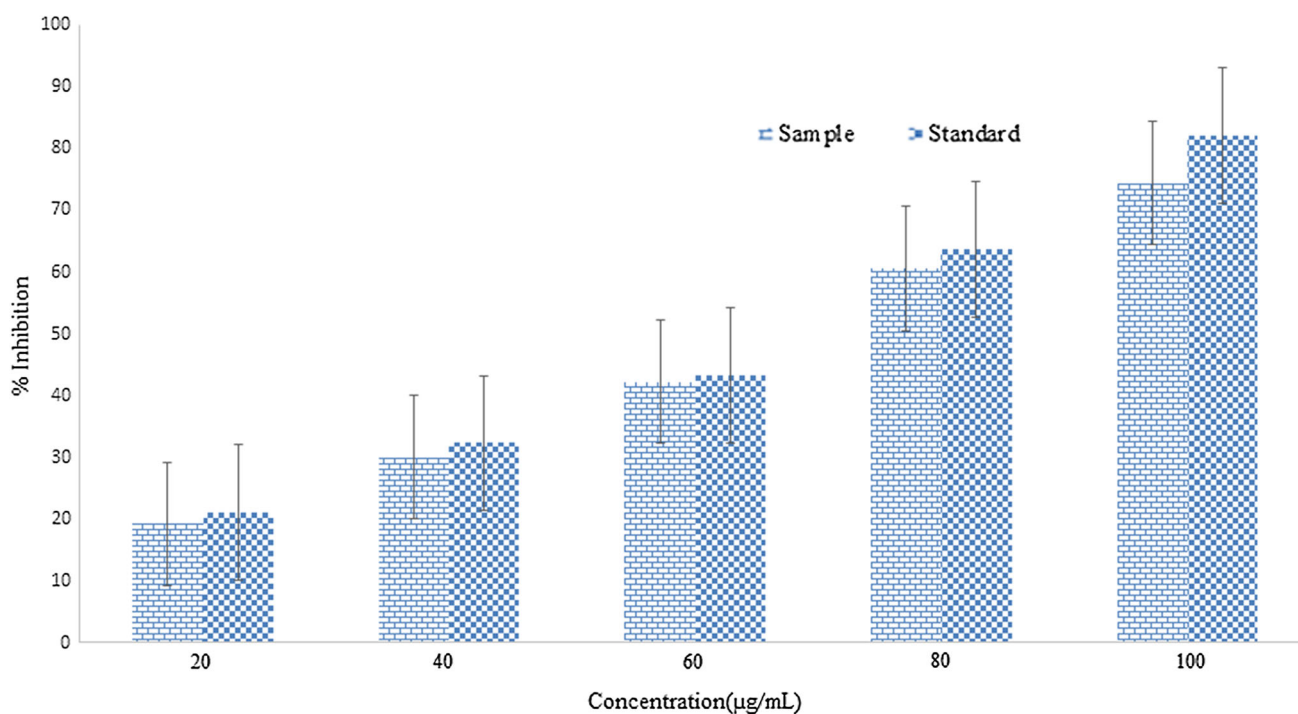


Fig. 7 DPPH radical scavenging activity

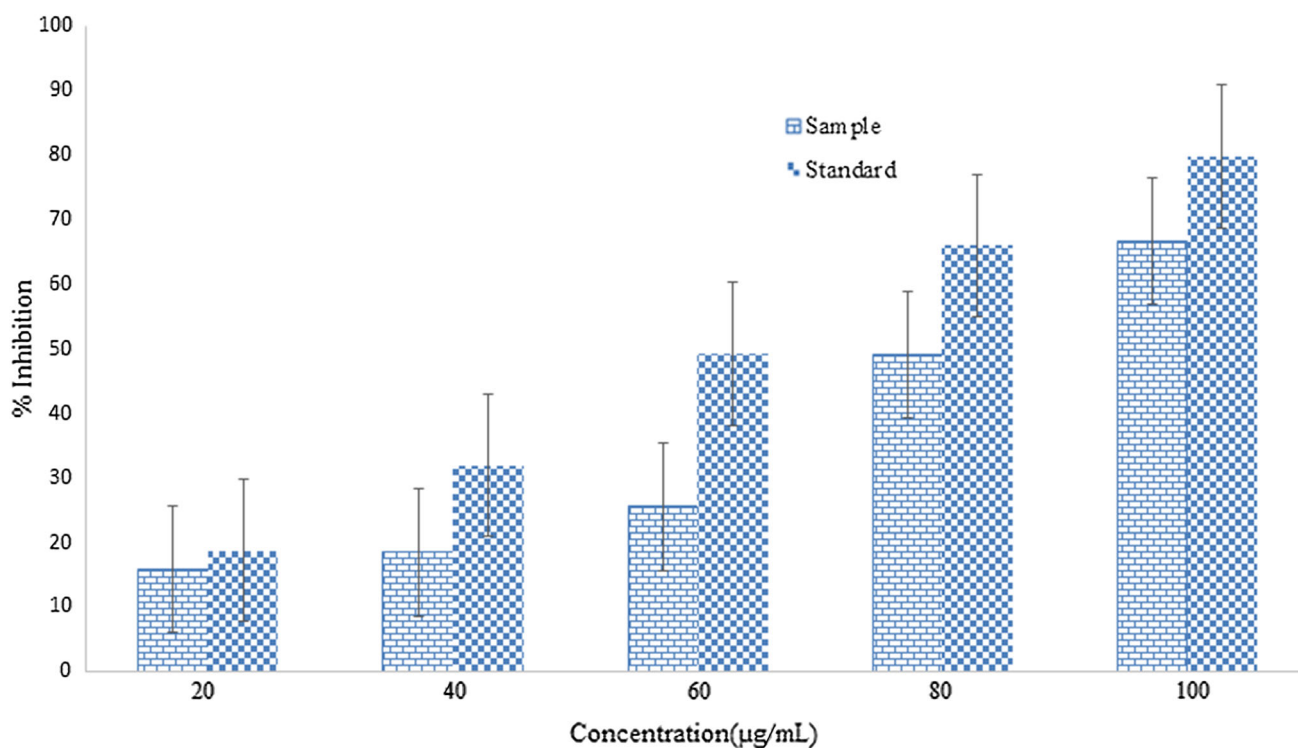


Fig. 8 Metal ion chelation activity

formation of Prussian blue colored complex. High absorbance value indicated the higher reducing power. The StNPs showed the absorbance values of 0.243 ± 0.003 , 0.266 ± 0.003 , 0.321 ± 0.002 , 0.349 ± 0.002 , and

0.385 ± 0.002 for the concentrations of 20 µg/mL, 40 µg/mL, 60 µg/mL, 80 µg/mL and 100 µg/mL, respectively. 100 µg/mL showed the higher absorbance value of 0.385 ± 0.002 at 700 nm. The antioxidant molecules

donate an electron to the free radical to neutralize it to make stable compounds. Figure 9 described the graphical representation of reducing power assay.

Alpha-Amylase Inhibition Assay

In vitro antidiabetic activity was studied using inhibitory effects of alpha-amylase with the standard drug acarbose for the comparison. Alpha amylase and alpha glucosidase are the two enzymes present in digestive tract which are responsible for the starch hydrolysis leads to the formation of monosaccharides. The standard curve of the inhibitory effects of StNPs and acarbose against alpha amylase showed the dose dependent activity ($R^2 = 0.9864$ and 0.9624). The highest inhibition activity of the StNPs showed $58.56 \pm 0.44\%$ at concentration of $100 \mu\text{g/mL}$ which was significant to that of standard which showed $68.58 \pm 0.38\%$ at the same concentration. The StNPs showed inhibition values of $19.02 \pm 0.40\%$, $32.42 \pm 0.26\%$, $41.82 \pm 0.32\%$, $48.33 \pm 0.46\%$, and $58.56 \pm 0.44\%$ for the concentrations of $20 \mu\text{g/mL}$, $40 \mu\text{g/mL}$, $60 \mu\text{g/mL}$, $80 \mu\text{g/mL}$, and $100 \mu\text{g/mL}$, respectively. The standard (acarbose) showed the inhibition values of $25.02 \pm 0.49\%$, $36.84 \pm 0.76\%$, $51.79 \pm 0.43\%$, $66.45 \pm 0.43\%$, and $68.58 \pm 0.38\%$ for the concentrations of $20 \mu\text{g/mL}$, $40 \mu\text{g/mL}$, $60 \mu\text{g/mL}$, $80 \mu\text{g/mL}$, and

$100 \mu\text{g/mL}$, respectively. The IC_{50} value was calculated from the standard curve of StNPs and it was found to be $80.98 \mu\text{g/mL}$. The IC_{50} was calculated from the standard curve of standard (acarbose) and it was found to be $60.45 \mu\text{g/mL}$. The Fig. 10 showed the graphical representation of alpha-amylase inhibition assay.

Glucose Uptake by Yeast Cells

The StNPs enhanced the glucose uptake in the yeast cells compared with the control (water). The amount of glucose uptake was determined by the presence of unused glucose present in the medium which was evaluated by a colorimetric DNS (dinitrosalicylic acid) method. The rate of glucose uptake in the yeast cells was presented in Table 1. The increase in the glucose uptake by the yeast cells was observed to be inversely proportional to the glucose concentration and was found to be decreased with increase in molar concentration of glucose. When the sample amount increases with increase in glucose concentration, reduces the glucose uptake in the yeast cells. This is due to the presence of high number of fibrous components present in the StNPs. It was reported that the stereospecific membrane carriers are responsible for sugar transport across the yeast cell membrane [34].

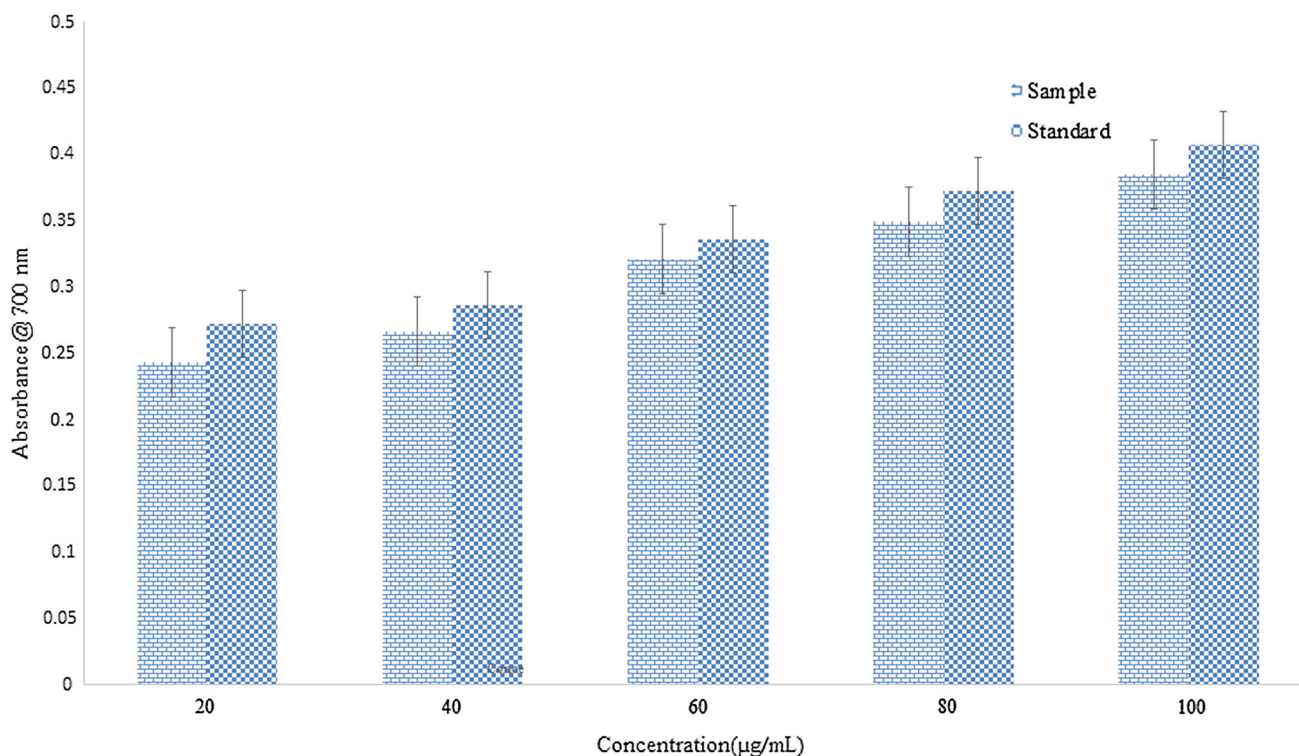


Fig. 9 Reducing power activity

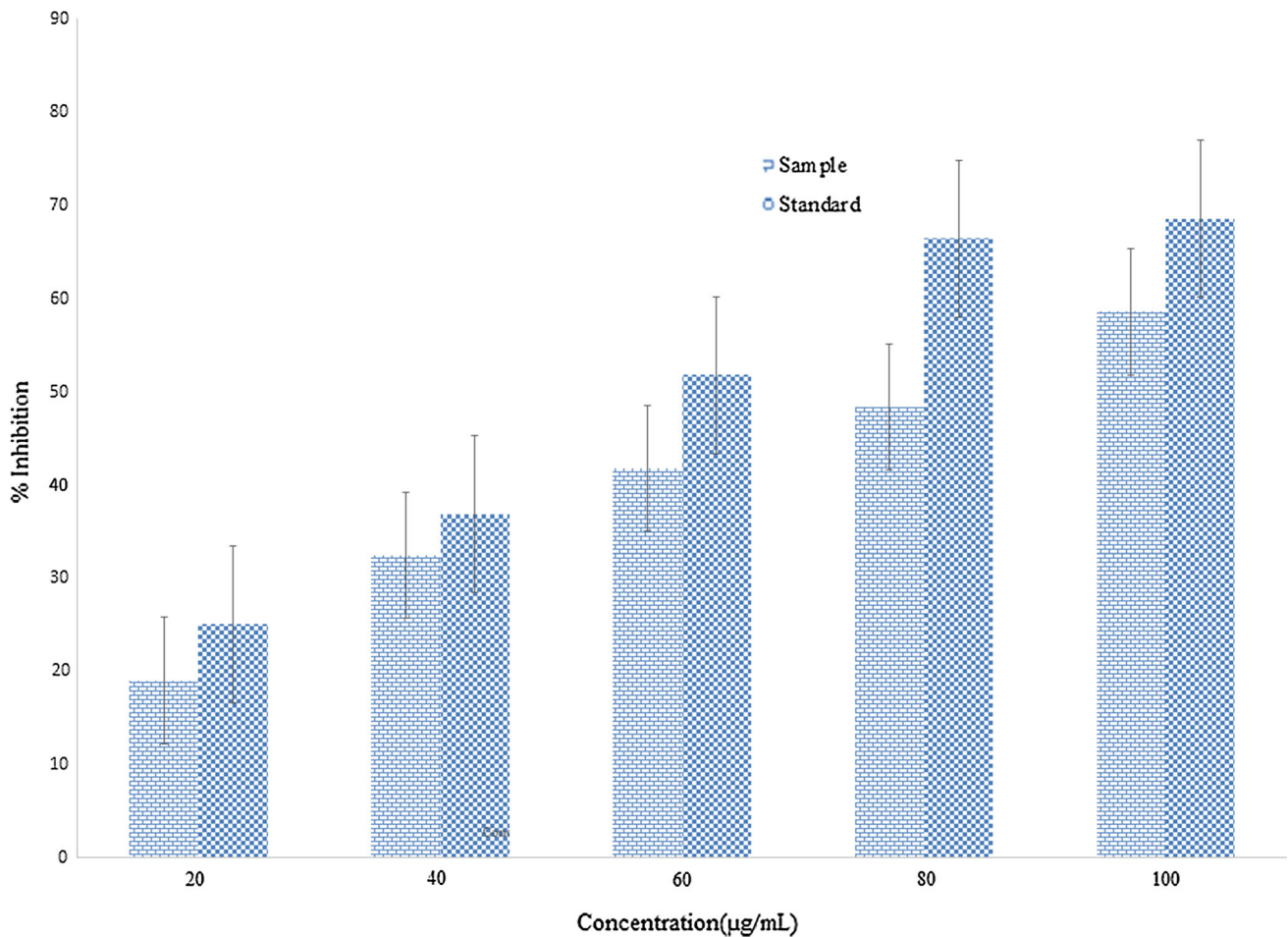


Fig. 10 Alpha-amylase inhibition assay

Table 1 Glucose uptake assay

Glucose concentration (mM/L)	Sample concentration (µg/mL)	Percentage of glucose uptake by yeast cells (%)
5	100	73
	200	59
	300	46
10	100	67
	200	52
	300	39
15	100	62
	200	48
	300	35

Conclusion

The present study concluded that the StNPs synthesized from the methanolic leaf extract of *G. sylvestre* had the potential inhibitory activity against diabetes though in vitro model. Since *G. sylvestre* possess various medicinal

properties, it can be used for vast biological applications. The methanolic extract proved to be the best solvent for the synthesis of StNPs. The synthesized StNPs were characterized by SEM, FTIR, XRD, PSA and EDS. The StNPs obtained were found to be ellipsoidal in shape with the average particle size of 19.8 nm. The XRD and FTIR

results showed the nature and functional groups presented in the StNPs. Six bioactive components were identified in the leaf extract by GC–MS analysis. Hence from the present study, it was concluded that the StNPs showed the highest potential antioxidant activity and antidiabetic activity which was determined by various antioxidant assays and antidiabetic assay.

Compliance with Ethical Standards

Conflict of interests The authors declare no conflict of interests.

References

- J. Jeevanandam, A. Barhoum, Y. S. Chan, A. Dufresne, and M. K. Danquah (2018). *Beilstein J. Nanotechnol.* **9**, 1050.
- S. Mishra, C. Keswani, P. C. Abhilash, L. F. Fraceto, and H. B. Singh (2017). *Front. Plant Sci.* **8**, 471.
- M. A. Gatoo, S. Naseem, M. Y. Arfat, A. M. Dar, K. Qasim, and S. Zubair (2014). *Biomed. Res. Int.* **2014**, 498420.
- Q. Abbas, M. Saleem, A. R. Phull, M. Rafiq, M. Hassan, K.-H. Lee, and S.-Y. Seo (2017). *Iran. J. Pharm. Res.* **16**, 760.
- N. Karimi, A. Chardoli, and A. Fattahi (2017). *Iran. J. Pharm. Res.* **16**, 1167.
- B. Miri, N. Motakef-Kazemi, S. A. Shojaosadati, and A. Morsali (2018). *Iran. J. Pharm. Res.* **17**, 1164.
- M. M. Or Rashid, M. S. Islam, M. A. Haque, M. A. Rahman, M. T. Hossain, and M. A. Hamid (2016). *Iran. J. Pharm. Res.* **15**, 591.
- S. Salari, S. Esmaeilzadeh Bahabadi, A. Samzadeh-Kermani, and F. Yousefzadei (2019). *Iran. J. Pharm. Res.* **18**, 430.
- K. S. Siddiqi, A. Husen, and R. A. K. Rao (2018). *J. Nanobiotechnol.* **16**, 14.
- S. H. Lee and B.-H. Jun (2019). *Int. J. Mol. Sci.* **20**, 865.
- H. Barabadi, K. Damavandi Kamali, F. Jazayeri Shoushtari, B. Tajani, M. A. Mahjoub, A. Alizadeh, and M. Saravanan (2019). *J. Clust. Sci.* **30**, 1375.
- S. K. Kulkarni Synthesis of nanomaterials—I (physical methods). in S. K. Kulkarni (ed.), *Nanotechnology: principles and practices* (Springer International Publishing, Cham, 2015), p. 55.
- H. Barabadi, F. Kobarfard, and H. Vahidi (2018). *Iran. J. Pharm. Res.* **17**, 87.
- R. Dobrucka (2017). *Iran. J. Pharm. Res.* **16**, 753.
- M. Maham and R. Karami-Osboo (2017). *Iran. J. Pharm. Res.* **16**, 462.
- T. Ramezani, M. Nabiuni, J. Baharara, K. Parivar, and F. Namvar (2019). *Iran. J. Pharm. Res.* **18**, 222.
- Z. Rezvani Amin, Z. Khashyarmanesh, B. S. Fazly Bazzaz, and Z. Sabeti Noghahi (2019). *Iran. J. Pharm. Res.* **18**, 210.
- R. K. Das, V. L. Pachapur, L. Lonappan, M. Naghdi, R. Pulicharla, S. Maiti, M. Cledon, L. M. A. Dalila, S. J. Sarma, and S. K. Brar (2017). *Nanotechnol. Environ. Eng.* **2**, 18.
- S. Menon, S. Rajeshkumar, and S. Venkat Kumar (2017). *Resour. Effic. Technol.* **3**, 516.
- Q. Li, Y. Niu, P. Xing, and C. Wang (2018). *Chin. Med.* **13**, 7.
- M. Swierczewska, H. S. Han, K. Kim, J. H. Park, and S. Lee (2016). *Adv. Drug Deliv. Rev.* **99**, 70.
- A. Hebeish, M. H. El-Rafie, M. A. El-Sheikh, and M. E. El-Naggar (2014). *J. Inorg. Organomet. Polym. Mater.* **24**, 515.
- A. American Diabetes (2010). *Diabetes Care* **33 Suppl 1**, S62.
- M. Syedy and K. S. Nama (2014). *Int. J. Pure Appl. Biosci.* **2**, 318.
- S. Anjali and S. Sheetal (2013). *J. Pharmacogn. Phytochem.* **2**, 22.
- O. O. Olubomehin, K. A. Abo, and E. O. Ajaiyeoba (2013). *J. Ethnopharmacol.* **146**, 811.
- T. C. Dinis, V. M. Maderia, and L. M. Almeida (1994). *Arch. Biochem. Biophys.* **315**, 161.
- M. S. Blois (1958). *Nature* **181**, 1199.
- T. Hatano, H. Kagawa, T. Yasuhara, and T. Okuda (1988). *Chem. Pharm. Bull.* **36**, 2090.
- V. P. Cirillo (1962). *J. Bacteriol.* **84**, 485.
- M. Oyaizu (1986). *Jpn. J. Nutr.* **44**, 307.
- S. Bel Haaj, A. Magnin, C. Petrier, and S. Boufi (2013). *Carbohydr. Polym.* **92**, 1625.
- S. Kalyani and D. Bandita (2014). *J. Med. Plants Stud.* **2**, 19.
- R. Pitchaipillai and T. Ponniah (2016). *Int. Biol. Biomed. J.* **2**, 171.

Publisher's Note Springer Nature remains neutral with regard to jurisdictional claims in published maps and institutional affiliations.